Translational Stroke Research (2019) 10:440–448
https://doi.org/10.1007/s12975-018-0670-7

ORIGINAL ARTICLE

Preconditioning in the Rhesus Macaque Induces a Proteomic Signature Following Cerebral Ischemia that Is Associated with Neuroprotection

Susan L. Stevens[1] · Tao Liu[2] · Frances Rena Bahjat[1] · Vladislav A. Petyuk[2] · Athena A. Schepmoes[2] · Ryan L. Sontag[2] · Marina A. Gritsenko[2] · Chaochao Wu[2] · Sheng Wang[2] · Anil K. Shukla[2] · Jon M. Jacobs[2] · Richard D. Smith[2] · Karin D. Rodland[2] · G. Alexander West[3] · Steven G. Kohama[4] · Christine Glynn[1] · Mary P. Stenzel-Poore[1]

Received: 16 July 2018 / Revised: 7 September 2018 / Accepted: 9 October 2018 / Published online: 19 October 2018

Abstract

Each year, thousands of patients are at risk of cerebral ischemic injury, due to iatrogenic responses to surgical procedures. Prophylactic treatment of these patients as standard care could minimize potential neurological complications. We have shown that protection of brain tissue, in a non-human primate model of cerebral ischemic injury, is possible through pharmacological preconditioning using the immune activator D192935. We postulate that preconditioning with D192935 results in neuroprotective reprogramming that is evident in the brain following experimentally induced cerebral ischemia. We performed quantitative proteomic analysis of cerebral spinal fluid (CSF) collected post-stroke from our previously published efficacy study to determine whether CSF protein profiles correlated with induced protection. Four groups of animals were examined: naïve animals (no treatment or stroke); animals treated with vehicle prior to stroke; D192935 treated and stroked animals, further delineated into two groups, ones that were protected (small infarcts) and those that were not protected (large infarcts). We found that distinct protein clusters defined the protected and non-protected animal groups, with a 16-member cluster of proteins induced exclusively in D192935 protected animals. Seventy percent of the proteins induced in the protected animals have functions that would enhance neuroprotection and tissue repair, including several members associated with M2 macrophages, a macrophage phenotype shown to contribute to neuroprotection and repair during ischemic injury. These studies highlight the translational importance of CSF biomarkers in defining mechanism and monitoring responses to treatment in development of stroke therapeutics.

Keywords Neuroprotection · Non-human primates · Stroke · Proteomics · Cerebral spinal fluid

Introduction

Neurological impairments, including ischemic stroke, are a major complication of life-saving endovascular and cardiac procedures [1, 2]. Advances in neuroimaging indicate that peri-procedural brain lesions can occur in up to 50% of patients undergoing these treatments [3–7]. Prophylactic treatment designed to protect brain tissue in the event of an ischemic episode may be extremely beneficial to these patients. Experimental models of ischemia have demonstrated that prophylactic protection of tissue is possible through an induced process known as preconditioning, in which exposure to a small dose of an otherwise harmful stimulus induces a protective state against a subsequent ischemic event [8]. In animal models, protection of multiple tissues (i.e., the brain, heart, and kidney) has been

Electronic supplementary material The online version of this article (https://doi.org/10.1007/s12975-018-0670-7) contains supplementary material, which is available to authorized users.

✉ Mary P. Stenzel-Poore
poorem@ohsu.edu

[1] Department of Molecular Microbiology and Immunology, Oregon Health & Science University, 3181 Sam Jackson Park Road, Portland, OR 97239, USA

[2] Biological Sciences Division, Pacific Northwest National Laboratory, Richland, WA, USA

[3] Houston Methodist Neurosurgery, Houston, TX, USA

[4] Division of Neuroscience, Oregon National Primate Research Center, Beaverton, OR, USA

demonstrated using brief ischemia as well as pharmacological induction of mild inflammation [9–12]. Transient remote ischemic preconditioning, using a tourniquet approach applied to the limbs to induce protection to the heart and kidney is already being tested in clinical trials [13–15]. Understanding these endogenous mechanisms of preconditioning-induced tissue protection would further translational development of potential prophylactic treatments for high-risk patients.

We have previously demonstrated protection against cerebral ischemic injury in murine and non-human primate (NHP) experimental models using pharmacological activation of toll-like receptor 9 (TLR9) to engage the innate immune response [9, 16, 17]. Extensive studies in our mouse model indicate that preconditioning prior to the ischemic insult results in an altered brain response to the injury. New genes are induced in the brain that indicate the activation of novel neuroprotective pathways that are not evident in the non-protected mouse brain [18]. Although we have demonstrated that an activator of TLR9 can provide significant protection in our NHP model of cerebral ischemia [9, 16], the molecular mechanisms associated with protection have not been elucidated. We hypothesize that, similar to the mouse, preconditioning of the NHP results in a reprogrammed response to ischemic injury contributes to protection. To explore further the molecular changes that accompany preconditioning-induced neuroprotection, we have examined cerebral spinal fluid (CSF) collected 7 days post occlusion from preconditioned and non-preconditioned NHPs, to determine whether preconditioning alters the brain's response to injury in this higher-order species and whether such changes are associated with neuroprotection.

As these studies make use of samples collected from our previous NHP efficacy study, the scope of this study was limited to tissue/resources available. Hence, the study was confined to examine evidence of a preconditioning-induced protective response in CSF collected from animals at the time of necropsy (7 days post occlusion). CSF is a repository of protein and has already proven to be an important site for biomarker analysis for many neurological disorders, such as Alzheimer's disease, multiple sclerosis, and stroke [19–23], thus providing an ideal medium for assessing potential changes in the brain associated with protection. In addition, at this late time point, evidence of a protected response is more likely to be manifested in protein differences, rather than transcriptional changes. Herein, we performed quantitative proteomics analysis using 10-plexed isobaric tandem mass tag (TMT-10) labeling [24] and off-line two-dimensional liquid chromatography coupled to tandem mass spectrometry (2D-LC-MS/MS), to assess the proteomic changes in the CSF.

Methods

Cerebral Spinal Fluid Samples

CSF samples were collected during a previously published study demonstrating the efficacy of a TLR9 agonist (D192935) to reduce cerebral ischemic injury in the non-human primate [16]. In brief, adult male rhesus macaques were treated with D192935 or vehicle 3 days prior to 60-min middle cerebral artery and anterior cerebral artery occlusion (MACAO). CSF was collected 7 days following MACAO (at necropsy) immediately centrifuged and clarified samples stored at − 80 °C for further analysis. Four groups were compared: (1) drug protected (DP)—D192935 treated followed by MACAO (small infarcts: group mean 1.36 ± 1.2% of whole brain Fig. 1; $n = 5$), (2) drug not protected (DNP)—D192935 treated followed by MACAO (large infarcts: group mean 6.35 ± 1.2% of whole brain Fig. 1; $n = 5$), (3) control (CNTL)—vehicle treated followed by MACAO (group mean 8.72 ± 1.1% of whole brain Fig. 1; $n = 5$), and (4) naïve—no treatment or surgery ($n = 4$).

Digestion of CSF Samples

Approximately 500 μL of each CSF sample was concentrated to ~ 100 μL using a Millipore Amicon Ultra-15 3000 MWCO filter (Fisher Scientific). Solid urea and 100 mM dithiothreitol were added to each sample to a final concentration of 8 M and 10 mM, respectively, and the samples were incubated at 37 °C for 1 h to denature and reduce the proteins, after which the samples were alkylated with 40 mM iodoacetamide for 1 h in the dark at 37 °C. The samples were diluted 10× with 50 mM

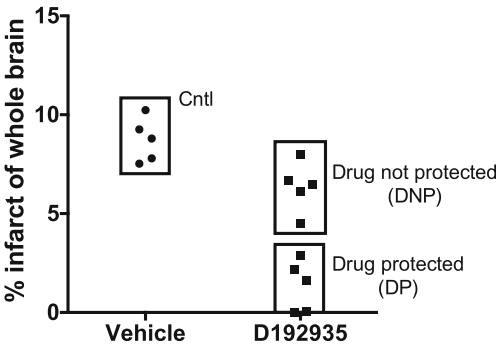

Fig. 1 Infarct size of the experimental study groups. D192935 or vehicle was administered via intramuscular injection to male NHPs 3 days prior to the onset of surgical occlusion as described in [16]. T2-weighted MR imaging was performed on day 2 following reperfusion and infarct size determined as percent of total brain. Data presented are a subset of animals, chosen based on infarct size, from previously published study [16]. Study groups are shown as CNTL: vehicle treated; drug not protected (DNP): D192935 treated with large infarcts (top box); drug protected (DP): D192935 treated with small infarcts (bottom box)

NH_4HCO_3, 10 mM $CaCl_2$, and digested with sequencing grade modified trypsin (Promega) for 3 h at 37 °C, using 1:50 trypsin-to-protein ratio. The samples were acidified with 10% trifluoroacetic acid and centrifuged at 14,000*g* before being desalted by C18 solid phase extraction (Supelco) and dried. Final peptide concentration was determined with BCA assay (Pierce).

TMT-10 Labeling and Fractionation

The TMT labeling was performed per manufacturer's instructions. A pooled reference was first created with equal contribution from each sample. This pooled reference sample and each individual sample were dried and dissolved in triethylammonium bicarbonate, before the TMT reagent prepared in anhydrous acetonitrile was added. The TMT-10 labeling scheme is shown in Supplementary Table 1. The reaction was incubated at room temperature for 90 min prior to termination with 5% hydroxylamine. Samples with different TMT labeling in the same TMT-10 experiment were combined, acidified, and desalted on C18 solid phase extraction column, followed by basic pH reversed-phase LC (bRPLC) fractionation and concatenation [25]. Mobile phases were as follows: (A) 10 mM ammonium formate, pH 10 and (B) 10 mM ammonium formate, 90% acetonitrile, pH 10. Sample separation was carried out at a flow rate of 0.5 mL/min using the following gradient (minute: B%): 0:0, 35:0, 41:10, 127:30, 137:42.5, 142:55, 147:100, 148:0, and 178:0. Fractions were collected from 48 to 164 min with equal intervals of 1.2 min, and the fractions were concatenated into 24 final fractions [25].

LC-MS/MS Analysis

The LC system was custom built using two Agilent 1200 nanoflow pumps, one Agilent 1200 capillary pump (Agilent Technologies) and a PAL autosampler (Leap Technologies). Reversed-phase columns were prepared in-house by slurry packing 3-μm Jupiter C18 (Phenomenex) into 40 cm × 360 μm o.d. × 75 μm i.d. fused silica column (Polymicro Technologies Inc.) using a 3-mm sol-gel frit for media retention. Trapping columns were prepared similarly by slurry packing 5-μm Jupiter C18 into a 4-cm length of 150-μm i.d. fused silica and fritted on both ends. Mobile phases consisted of 0.1% formic acid in water (A) and 0.1% formic acid in acetonitrile (B) operated at 300 nL/min with a gradient profile as follows (minutes: %B); 0:5, 2:8, 20:12, 75:35, 97:60, 100:85. Samples were injected and analyzed using the capillary RPLC system coupled online to a Q Exactive Plus Orbitrap mass spectrometer (Thermo Scientific). Full MS spectra (400–2000 *m*/*z*) were acquired with a resolution of 35,000. Top-10 most intensive precursor ions were selected for MS/MS using higher energy collision dissociation (HCD) with a normalized collision energy of 30%, and the product ions were detected in the Orbitrap with a resolution of 35,000.

Protein Identification and Quantification

The MS raw data were searched against the UniProt macaque protein database using MS-GF+ [26]. The searching parameters are as follows: precursor ion mass tolerance (± 10 ppm), partial tryptic specificity, dynamic oxidation of Met (15.9949 Da), static alkylation on Cys (57.0215 Da), and static TMT labeling on the N-terminal and Lys (229.1629 Da). The search results were filtered to obtain a false identification rate of < 1% at peptide level.

The intensities of all ten TMT reporter ions were extracted using MASIC software [27]. The reporter ion intensities from different scans and/or different fractions corresponding to the same protein were summed. Relative protein abundance was then calculated as the ratio of sample abundance to abundance of the pooled reference (i.e., sample/reference) and log2 transformed to obtain final relative expression values. This allows comparison of relative protein abundances across the entire sample set with minimum variation from each TMT-10 experiment. The strategy of using a common "internal" reference for merging different multiplexed experiments in isobaric labeling analysis has been demonstrated recently as a highly effective and reliable way for large-scale quantitative proteomics analysis [28, 29].

Statistical and Bioinformatics Analyses

To correct for potential differences in sample loading in the same TMT-10 experiment, the median log2 relative abundance of the proteins present in each sample was computed and re-centered. Moderated 3-group (CNTL, DP, and DNP) ANOVA was performed using the limma package [30]. The null hypothesis is no difference between the different sample groups. To correct for multiplicity of hypothesis testing, individual protein values were adjusted by converting to *q* values using a corresponding R package [31]. Principle component analysis (PCA) and unsupervised hierarchical clustering were performed in R. Clustering was performed on proteins that were differentially expressed between DNP and DP with FDR < 0.2. Distance metric was based on Pearson correlation. Specifically, distance = (1 − cor) / 2, making a highly positive correlation (cor = 1), have a distance 0 and inversely correlated (− 1) have a distance 1. The macaque UniProt IDs were linked to human orthologues using InParanoid database [32].

Results

Experimental Groups

In our previously published efficacy study, we found that the TLR9 agonist, D192935 provided significant protection when administered via intramuscular injection 3 days prior to surgically induced cerebral ischemia [16]. Although significant protection was observed in the group of animals treated with D192935, there was a range of infarct sizes noted, that suggested that not all animals responded to the treatment equally (range from 0 to 9.2% of total brain). Based on the heterogeneity of the NHP population, the variable response was anticipated as it has been reported that TLR9 immune responses in humans vary between individuals [33–35]. In fact, D192935 is a mixture of three oligodeoxynucleotide sequences combined to provide the broadest activation between human individuals [16, 33]. To determine whether key pathways of neuroprotection could be identified in protected animals, we compared proteomic profiles in the CSF collected 7 days following MACAO from five animals that received D192935 and exhibited small infarcts (DP; range 0 to 2.9%, mean 1.36 ± 1.2% of total brain; Fig. 1), five animals that received D192935 and failed to be protected (DNP; large infarcts; range 4.5 to 8.0%, mean 6.35 ± 1.2% of total brain; Fig. 1), and five animals treated with vehicle (CNTL; range 7.5 to 10.2%, mean 8.72 ± 1.1% of total brain; Fig. 1) as well as a group of naïve animals ($n = 4$): non-treated and not exposed to ischemia.

Proteomic Analysis

The multiplexed TMT-10 labeling method coupled to offline 2D-LC-MS/MS allowed for precise quantitative analysis of the individual CSF samples while achieving comprehensive proteome coverage. A total of 28,641 peptides were identified in the CSF samples (Supplementary Table 2), covering 4029 proteins (Supplementary Table 3). Of these proteins identified, 2125 had complete data for all 19 samples. PCA analysis using these proteins showed complete separation of the DP and DNP groups, and that the DNP group is more similar to the CNTL group (Fig. 2). In addition, the naïve and DP groups show a slight overlap, but still delineate into distinct groups (Fig. 2). We were able to map 2751 of the macaque proteins to human orthologues using the InParanoid database (Supplementary Table 4), which were used for further statistical and pathway analyses.

Hierarchical Clustering

Clustering the individual animals based on expression levels of the proteins identified as differentially regulated in the CNS by ANOVA (adjusted p value < 0.05; Supplementary Table 5) clearly differentiates the naïve and DP ("minimal damage" group) form the CNTL and DNP ("damage" group; Fig. 3-point A). Proteins were clustered based on differential expression between the DNP and DP (FDR < 0.2), and two clusters were identified (Fig. 3-left side dendrogram). The hallmark of the minimal damage animal cluster appears to be low expression of the proteins associated with the orange protein cluster. The animals in the damage cluster have high expression levels of proteins in the orange cluster suggesting that these proteins might be related to the evolution of injury (Supplementary Table 6). The minimal damage cluster is further delineated by increased expression of proteins in the green cluster, separating all five DP animals from the naïve group (Fig. 3-point B). Interestingly, similar to the control non-stroked animals (CNTL), the animals in the damage cluster have low levels of proteins in the green cluster. The increased expression of the proteins in the green cluster in the DP animal group compared to the other animal groups suggests that these proteins may be associated with neuroprotection (Fig. 3-left side dendrogram; Table 1). The delineation of groups by their proteomic expression profiles indicates that proteins in the CNS reflect physiological differences between the groups and may provide insight into protein profiles involved in injury and neuroprotection/repair.

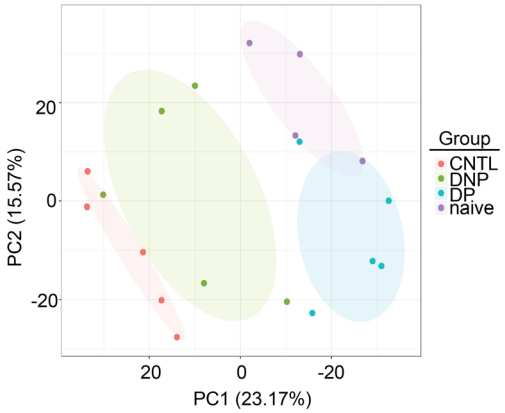

Fig. 2 Principal component analysis delineates the study groups. PCA using the 2125 proteins which had complete data sets for all 19 samples. Shaded ellipses denote the different experimental groups

Proteins in the Neuroprotective Cluster

Of the 16 proteins identified in the neuroprotective cluster (green), six are significantly increased compared to naïve animals: Adiponectin (ADIPOQ), Mannose Binding Lectin 2 (MBL2), Sex hormone-binding globulin (SHBG), Coagulation Factor XIII A chain (F13A1), Lysyl oxidase like 1 (LoxL1), and Myosin heavy chain 2 (MYH2) (Fig. 4). In addition, all but one, Heparan sulfate 6-O Sulfotransferase 1

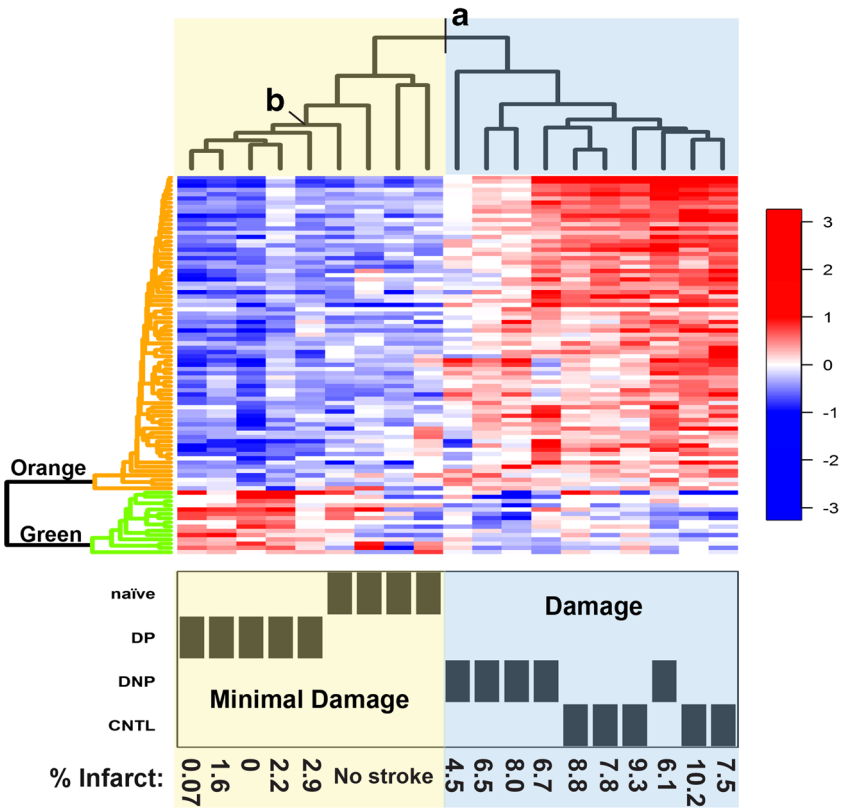

Fig. 3 Heatmap of hierarchical clustering of differentially regulated proteins expressed in the CNS. Heatmap of individual protein expression levels (key on right) with hierarchical clustering performed using R. Top dendrogram: individual animals were clustered based on the proteomic expression profiles of proteins identified as differentially regulated by ANOVA (adjusted p value < 0.05). Animal groups and infarct size of individual animals are shown at the bottom. **a** Point of separation between minimal damage and damage groups. **b** Point that differentiates DP group from naïve animals. Left dendrogram: clustering of proteins delineates into two distinct cluster groups: Orange: high levels in the damaged animal groups and green: high levels in the DP minimal damage group

(HS6ST1), of the other 10 proteins also show a trend toward increased expression compared to naïve animals (Supplemental Fig. 1). The fact that these proteins are increased compared to naïve animals suggests that they may define and/or contribute to a neuroprotective state. Pearson correlation analysis of individual animals found that infarct size was negatively correlated with each of the six significantly increased proteins.

Discussion

We have previously shown that the immune activator D192935 provides significant protection against ischemia-reperfusion injury in the NHP [16]. In the studies reported here, CSF collected from the original study animals at necropsy was used to determine whether proteins in the CSF reflect a change in the response to injury that may highlight mechanisms of protection. Our studies show that clustering of animals based on protein expression levels in the CSF following ischemic injury delineated the NHPs into those with minimal injury and those with significant injury. Of note, two distinct clusters of proteins were identified, one cluster being upregulated in the animals with minimal injury (DP) and the other increased in the animals with significant injury (DNP and CNTL). Proteins in these clusters may represent pathways in the brain associated with neuroprotection and damage respectively, highlighting potential targets for further therapeutic development.

Our perspective that CSF could act as a window into the state of the brain is based on the fact that CSF circulates through the central nervous system moving molecules throughout the brain and removing metabolic waste, making it an ideal repository for protein regulators and indicators of brain function. During stroke, leakage of proteins from the periphery occurs through degradation of the blood brain barrier (BBB). Such leakage can contribute to the protein profile of the CSF and influence responses directly in the brain. Although we did not measure BBB integrity in these studies, BBB leakage likely contributes significantly to the proteins identified in the CSF following stroke. In the damaged animals, BBB degradation would be expected to be severe and would allow peripheral proteins to leak into the CSF contributing to the orange cluster of proteins which are increased in these animals. However, it is noteworthy that proteins in the green cluster are increased in the protected animals and not in the damaged animals. This indicates that the proteins detected in the CSF are not simply a non-specific influx that occurred due to potential BBB leakage because these proteins are not increased in the more severely injured animals. Whether the proteins in the green cluster originate in the brain or extravasate from the periphery,

Table 1 Neuroprotective potential of proteins identified in the green cluster

UniProt ID	Gene symbol human	Protein name	Potential neuroprotective functions	Refs.
Q15848	ADIPOQ	Adiponectin	Primes transition to M2 macrophages, reduces oxidative stress, shown to be protective in mouse models of cerebral ischemia	[42, 48, 49]
P00488	F13A1	Coagulation factor XIII A chain	M2 macrophage marker, increases macrophage phagocytosis capability	[39]
O60243	HS6ST1	Heparan sulfate 6-O sulfotransferase 1	Neuronal axon patterning	[57]
Q08397	LOXL1	Lysyl oxidase like 1	Stabilizes the extracellular matrix	[59]
P11226	MBL2	Mannose binding lectin	Immunosuppressive, binds apoptotic and necrotic cells to facilitate macrophage phagocytosis and induces macrophage secretion of immunosuppressive cytokines.	[43, 44]
Q9H8L6	MMRN2	Multimerin 2	Angiogenesis	[56]
P02763	ORM1/ AGP1	Orosomucoid 1/alpha-1-acid glycoprotein 1	Immunosuppression, increases CD163 a M2 macrophage marker	[41]
Q14435	GALNT3	Polypeptide N-acetylgalactosaminyltransferase 3	Protects endothelial cells	[58]
P04278	SHBG	Sex hormone-binding globulin	Glucose metabolism	[50]
Q9NY15	STAB1	Stabilin 1	M2 macrophage marker, increases macrophage phagocytosis capability. Angiogenesis	[40, 55]
O95183	VAMP5	Vesicle associated membrane protein 5	Involved in vesicle transport of the glucose transporter, GLUT4	[52]
P04217	A1BG	Alpha-1-B glycoprotein		
P01591	JCHAIN	Immunoglobulin J chain		
P15814	IGLL1	Immunoglobulin lambda like polypeptide 1		
Q9UKX2	MYH2	Myosin heavy chain 2		
Q5T1S8	NCMAP	Non-compact myelin-associated protein		

their exclusive increase in the protected animals suggests that they may represent a mechanism of protection engaged by D192935 preconditioning.

We found a significant number of proteins increased in the CSF 7 days post the ischemic event, indicating that even at this late time point, the brain continues to respond to the injury. One limitation of our study is that at this late time point, the predominant responses are likely reparative in nature and that acute protective responses may be missed. Thus, although our data does not address a potential role for acute response in the protected animals, it does highlight potential pathways that may have been initiated in response to the stroke in the protected animals. The proteomic profiles of the CSF proteins define two clusters of proteins that differentiate the animal groups, one associated with the protective phenotype while the other corresponds to the damage phenotype. Eleven of the 16 proteins identified in the neuroprotective cluster have known functions that could contribute to neuroprotection. Four of these, adiponectin, F13A1, ORM1/AGP1, and STAB1, are directly associated with type 2 immunosuppressive macrophages (M2), a cell type that has been shown to be neuroprotective in animal models of stroke and in clinical trials (reviewed in [36]). Amantea and colleagues found that azithromycin, an immunomodulatory molecule, reduced ischemic injury in a mouse cerebral ischemia model through the polarization of macrophages to an M2 phenotype [37]. In humans, a phase I/II clinical trial found that stroke patients treated with autologous M2 macrophages had better neurological recovery, further supporting a protective role of these cells in reduction of stroke injury [38]. F13A1 and STAB1 are surface markers of M2 macrophages while ORM1 has been shown to induce the expression of CD163, another marker of M2 macrophages [39–41]. Adiponectin primes the transition of human monocytes into M2 macrophages representing a key modulator in this immunosuppressive response [42]. Another protein induced in this cluster, MBL2, is also immunosuppressive and may contribute to M2 transitions as it has been reported to bind apoptotic and necrotic cells, facilitating phagocytosis, and in the process directly interacting with macrophage receptors to alter cytokine expression, including suppression of pro-inflammatory cytokines (IL1a, IL1b) and the enhancement of anti-inflammatory cytokines, IL10 and IL1ra [43, 44], both of which are markers of M2 macrophages [45] and have been shown to reduce stroke injury [46, 47].

In addition to immunosuppressive activities, adiponectin has been shown to protect against cerebral ischemic injury in the mouse through modulation of

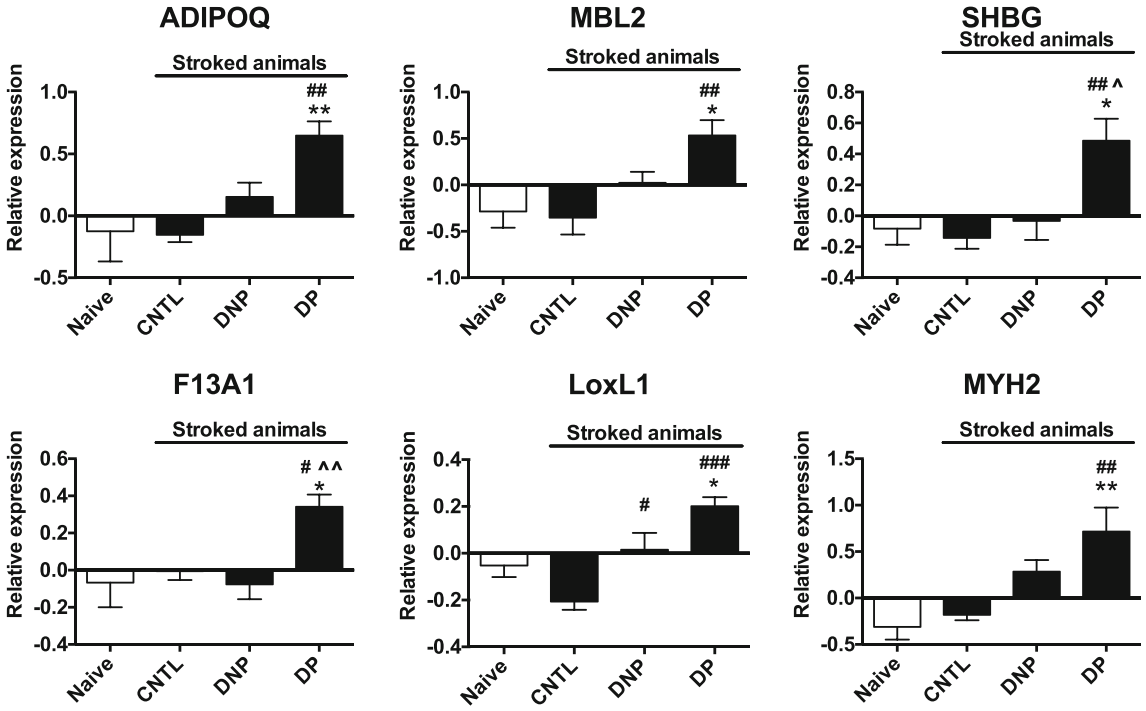

Fig. 4 Proteins with increased expression in drug-protected animals. Proteins with significant increase in expression in the DP group compared to naïve animals. Data are graphed as group means of the final relative expression values (log 2 transformation of the ratio of sample abundance to abundance of the pooled reference) ± SEM. One-way ANOVA with Tukey's multiple comparison post-hoc analysis $^{*}p < 0.05$, $^{**}p < 0.01$ vs naïve; $^{\#}p < 0.05$, $^{\#\#}p < 0.01$, $^{\#\#\#}p < 0.001$ vs CNTL; $^{\wedge}p < 0.05$, $^{\wedge\wedge}p < 0.01$ vs DNP

endothelial nitric oxide and through reduction of oxidative stress [48, 49], demonstrating other potential routes to neuroprotection. Glucose utilization can be optimized by adiponectin as well as SHBG which is associated with glucose metabolism and VAMP5 which is linked to glucose transporters [50–52]. Of note, ADIPOQ has been shown to regulate SHBG [53] and was grouped with SHBG and MBL2 in an associative network of genes connecting four disease states (pre-eclampsia, diabetes mellitus, gestational diabetes, and obesity) [54].

Along with the proteins associated with M2 macrophages, a number of other proteins that are differentially regulated in these animals appear to be involved in reparative responses that may be important in recovery from ischemic damage. For example, two proteins, MMRN2 and STAB1, are involved in modulating angiogenesis [55, 56] and HS6ST1 is involved in neuronal axon patterning [57]. In addition, GALNT3 promotes endothelial survival [58] and LOXL1 crosslinks collagen to stabilize the extracellular matrix and promote vessel wall integrity [59], all of which could contribute to reducing ischemic injury and promoting tissue repair. Thus, at least nine of the 11 proteins with known functions are associated with potential reparative responses as anticipated at this late time point.

Interestingly, six of the proteins in the neuroprotective cluster are significantly increased over the naïve animals as well as showing no induction in the non-protected animals. The increase compared to naïve animals may indicate that the protein levels of these in the CSF are upregulated in response to the ischemic injury and are not simply representing baseline expression levels that were suppressed in the non-protected animals. This may indicate a reprogrammed response to the injury that supports a neuroprotective environment, reducing the impact of ischemia and promoting recovery. It should be noted that we do not have CSF collected from animals that were treated with D192935 without the secondary stroke challenge. Thus, we cannot rule out that D192935 treatment alone, 10 days prior to the collection of CSF, induced these proteins independent of the stroke event and that in the non-protected animals where these proteins are not increased, a secondary suppression event inhibited their expression post-stroke.

These studies indicate the biomarker potential of the CSF as a way to monitor therapeutic effects in the brain, aiding in the translational development of candidate neuroprotectants. In addition, our studies further our knowledge of the potential mechanism of D192935-preconditioning-induced neuroprotection, indicating that immunosuppressive M2 macrophages may play a role in reparative efforts following ischemic injury. Understanding the endogenous mechanisms of preconditioning-induced tissue protection will help in the development of prophylactic treatments against ischemic injury for patients undergoing high-risk surgical procedures.

Acknowledgements The proteomics work described herein was performed in the Environmental Molecular Sciences Laboratory, a U.S. Department of Energy (DOE) national scientific user facility located at PNNL in Richland, Washington. PNNL is a multi-program national laboratory operated by Battelle Memorial Institute for the DOE under Contract DE-AC05-76RL01830.

Funding This work was supported by National Institutes of Health grants NS064953 (MSP, SGK), OD011092 (SGK), and P41GM103493 (RDS).

Compliance with Ethical Standards

Conflict of Interest All authors declare that they have no conflict of interest.

Ethical Approval All applicable international, national, and/or institutional guidelines for the care and use of animals were followed. This article does not contain any studies with human participants performed by any of the authors.

References

1. Bonati LH, Jongen LM, Haller S, Flach HZ, Dobson J, Nederkoorn PJ, et al. New ischaemic brain lesions on MRI after stenting or endarterectomy for symptomatic carotid stenosis: a substudy of the International Carotid Stenting Study (ICSS). Lancet Neurol. 2010;9:353–62.
2. Sun X, Lindsay J, Monsein LH, Hill PC, Corso PJ. Silent brain injury after cardiac surgery: a review: cognitive dysfunction and magnetic resonance imaging diffusion-weighted imaging findings. J Am Coll Cardiol. 2012;60:791–7.
3. Bendszus M, Stoll G. Silent cerebral ischaemia: hidden fingerprints of invasive medical procedures. Lancet Neurol. 2006;5:364–72.
4. Kahlert P, Al-Rashid F, Dottger P, Mori K, Plicht B, Wendt D, et al. Cerebral embolization during transcatheter aortic valve implantation: a transcranial Doppler study. Circulation. 2012;126:1245–55.
5. Rosenkranz M, Gerloff C. New ischemic brain lesions after carotid artery stenting. J Cardiovasc Surg. 2013;54:93–9.
6. Shibazaki K, Iguchi Y, Kimura K, Ueno Y, Inoue T. New asymptomatic ischemic lesions on diffusion-weighted imaging after cerebral angiography. J Neurol Sci. 2008;266:150–5.
7. Sun S, Zhang X, Tough DF, Sprent J. Type I interferon-mediated stimulation of T cells by CpG DNA. J Exp Med. 1998;188:2335–42.
8. Dirnagl U, Simon RP, Hallenbeck JM. Ischemic tolerance and endogenous neuroprotection. Trends in Neuroscience. 2003;26:248–54.
9. Bahjat FR, Williams-Karnesky RL, Kohama SG, West GA, Doyle KP, Spector MD, et al. Proof of concept: pharmacological preconditioning with a Toll-like receptor agonist protects against cerebrovascular injury in a primate model of stroke. J Cereb Blood Flow Metab. 2011;31:1229–42.
10. Brown JM, Grosso MA, Terada LS, Whitman GJ, Banerjee A, White CW, et al. Endotoxin pretreatment increases endogenous myocardial catalase activity and decreases ischemia-reperfusion injury of isolated rat hearts. Proc Natl Acad Sci U S A. 1989;86:2516–20.
11. Dave KR, Saul I, Prado R, Busto R, Perez-Pinzon MA. Remote organ ischemic preconditioning protect brain from ischemic damage following asphyxial cardiac arrest. Neurosci Lett. 2006;404:170–5.
12. Packard AE, Hedges JC, Bahjat FR, Stevens SL, Conlin MJ, Salazar AM, et al. Poly-IC preconditioning protects against cerebral and renal ischemia-reperfusion injury. J Cereb Blood Flow Metab. 2012;32:242–7.
13. Hausenloy DJ, Mwamure PK, Venugopal V, Harris J, Barnard M, Grundy E, et al. Effect of remote ischaemic preconditioning on myocardial injury in patients undergoing coronary artery bypass graft surgery: a randomised controlled trial. Lancet. 2007;370:575–9.
14. Hausenloy DJ, Kharbanda R, Rahbek Schmidt M, Møller UK, Ravkilde J, Okkels Jensen L, et al. Effect of remote ischaemic conditioning on clinical outcomes in patients presenting with an ST-segment elevation myocardial infarction undergoing primary percutaneous coronary intervention. Eur Heart J. 2015;36:1846–8.
15. Meybohm P, Bein B, Brosteanu O, Cremer J, Gruenewald M, Stoppe C, et al. A multicenter trial of remote ischemic preconditioning for heart surgery. N Engl J Med. 2015;373:1397–407.
16. Bahjat FR, West GA, Kohama SG, Glynn C, Urbanski HF, Hobbs TR, et al. Preclinical development of a prophylactic neuroprotective therapy for the preventive treatment of anticipated ischemia-reperfusion injury. Transl Stroke Res. 2017;8:322–33.
17. Stevens SL, Ciesielski TM, Marsh BJ, Yang T, Homen DS, Boule JL, et al. Toll-like receptor 9: a new target of ischemic preconditioning in the brain. J Cereb Blood Flow Metab. 2008;28:1040–7.
18. Stevens SL, Leung PY, Vartanian KB, Gopalan B, Yang T, Simon RP, et al. Multiple preconditioning paradigms converge on interferon regulatory factor-dependent signaling to promote tolerance to ischemic brain injury. J Neurosci. 2011;31:8456–63.
19. Aluise CD, Sowell RA, Butterfield DA. Peptides and proteins in plasma and cerebrospinal fluid as biomarkers for the prediction, diagnosis, and monitoring of therapeutic efficacy of Alzheimer's disease. Biochim Biophys Acta. 1782;2008:549–58.
20. Novakova L, Axelsson M, Khademi M, Zetterberg H, Blennow K, Malmeström C, et al. Cerebrospinal fluid biomarkers as a measure of disease activity and treatment efficacy in relapsing-remitting multiple sclerosis. J Neurochem. 2017;141:296–304.
21. Jung CS, Lange B, Zimmermann M, Seifert V. CSF and serum biomarkers focusing on cerebral vasospasm and ischemia after subarachnoid hemorrhage. Stroke Res Treat. 2013;2013:560305.
22. Mertens JC, Leenaerts D, Brouns R, Engelborghs S, Ieven M, De Deyn PP, et al. Procarboxypeptidase U (proCPU, TAFI, proCPB2) in cerebrospinal fluid during ischemic stroke is associated with stroke progression, outcome and blood-brain barrier dysfunction. J Thromb Haemost. 2018;16:342–8.
23. Zhang Y, Fan F, Zeng G, Zhou L, Zhang Y, Zhang J, et al. Temporal analysis of blood-brain barrier disruption and cerebrospinal fluid matrix metalloproteinases in rhesus monkeys subjected to transient ischemic stroke. J Cereb Blood Flow Metab. 2017;37:2963–74.
24. Thompson A, Schäfer J, Kuhn K, Kienle S, Schwarz J, Schmidt G, et al. Tandem mass tags: a novel quantification strategy for comparative analysis of complex protein mixtures by MS/MS. Anal Chem. 2003;75:1895–904.
25. Wang Y, Yang F, Gritsenko MA, Wang Y, Clauss T, Liu T, et al. Reversed-phase chromatography with multiple fraction concatenation strategy for proteome profiling of human MCF10A cells. Proteomics. 2011;11:2019–26.
26. Kim S, Pevzner PA. MS-GF+ makes progress towards a universal database search tool for proteomics. Nat Commun. 2014;5:5277.
27. Monroe ME, Shaw JL, Daly DS, Adkins JN, Smith RD. MASIC: a software program for fast quantitation and flexible visualization of chromatographic profiles from detected LC-MS(/MS) features. Comput Biol Chem. 2008;32:215–7.
28. Mertins P, Mani DR, Ruggles KV, Gillette MA, Clauser KR, Wang P, et al. Proteogenomics connects somatic mutations to signalling in breast cancer. Nature. 2016;534:55–62.

29. Zhang H, Liu T, Zhang Z, Payne SH, Zhang B, McDermott JE, et al. Integrated proteogenomic characterization of human high-grade serous ovarian cancer. Cell. 2016;166:755–65.
30. Ritchie ME, Phipson B, Wu D, Hu Y, Law CW, Shi W, et al. Limma powers differential expression analyses for RNA-sequencing and microarray studies. Nucleic Acids Res. 2015;43:e47.
31. Storey JD, Tibshirani R. Statistical significance for genomewide studies. Proc Natl Acad Sci U S A. 2003;100:9440–5.
32. Sonnhammer EL, Östlund G. InParanoid 8: orthology analysis between 273 proteomes, mostly eukaryotic. Nucleic Acids Res. 2015;43:D234–9.
33. Leifer CA, Verthelyi D, Klinman DM. Heterogeneity in the human response to immunostimulatory CpG oligodeoxynucleotides. J Immunother. 2003;26:313–9.
34. Hartmann G, Weeratna RD, Ballas ZK, Payette P, Blackwell S, Suparto I, et al. Delineation of a CpG phosphorothioate oligodeoxynucleotide for activating primate immune responses in vitro and in vivo. J Immunol. 2000;164:1617–24.
35. Bohle B, Orel L, Kraft D, Ebner C. Oligodeoxynucleotides containing CpG motifs induce low levels of TNF-alpha in human B lymphocytes: possible adjuvants for Th1 responses. J Immunol. 2001;166:3743–8.
36. Kanazawa, M., Ninomiya, I., Hatakeyama, M., Takahashi, T., and Shimohata, T. Microglia and monocytes/macrophages polarization reveal novel therapeutic mechanism against stroke. Int J Mol Sci 2017;18.
37. Amantea D, Certo M, Petrelli F, Tassorelli C, Micieli G, Corasaniti MT, et al. Azithromycin protects mice against ischemic stroke injury by promoting macrophage transition towards M2 phenotype. Exp Neurol. 2016;275(Pt 1):116–25.
38. Chernykh ER, Shevela EY, Starostina NM, Morozov SA, Davydova MN, Menyaeva EV, et al. Safety and therapeutic potential of M2 macrophages in stroke treatment. Cell Transplant. 2016;25:1461–71.
39. Soendergaard C, Kvist PH, Seidelin JB, Pelzer H, Nielsen OH. Systemic and intestinal levels of factor XIII-A: the impact of inflammation on expression in macrophage subtypes. J Gastroenterol. 2016;51:796–807.
40. Palani S, Maksimow M, Miiluniemi M, Auvinen K, Jalkanen S, Salmi M. Stabilin-1/CLEVER-1, a type 2 macrophage marker, is an adhesion and scavenging molecule on human placental macrophages. Eur J Immunol. 2011;41:2052–63.
41. Komori H, Watanabe H, Shuto T, Kodama A, Maeda H, Watanabe K, et al. α(1)-Acid glycoprotein up-regulates CD163 via TLR4/CD14 protein pathway: possible protection against hemolysis-induced oxidative stress. J Biol Chem. 2012;287:30688–700.
42. Lovren F, Pan Y, Quan A, Szmitko PE, Singh KK, Shukla PC, et al. Adiponectin primes human monocytes into alternative anti-inflammatory M2 macrophages. Am J Physiol Heart Circ Physiol. 2010;299:H656–63.
43. Fraser DA, Bohlson SS, Jasinskiene N, Rawal N, Palmarini G, Ruiz S, et al. C1q and MBL, components of the innate immune system, influence monocyte cytokine expression. J Leukoc Biol. 2006;80:107–16.
44. Ogden CA, de Cathelineau A, Hoffmann PR, Bratton D, Ghebrehiwet B, Fadok VA, et al. C1q and mannose binding lectin engagement of cell surface calreticulin and CD91 initiates macropinocytosis and uptake of apoptotic cells. J Exp Med. 2001;194:781–95.
45. Rőszer T. Understanding the mysterious M2 macrophage through activation markers and effector mechanisms. Mediat Inflamm. 2015;2015:816460.
46. de Bilbao F, Arsenijevic D, Moll T, Garcia-Gabay I, Vallet P, Langhans W, et al. In vivo over-expression of interleukin-10 increases resistance to focal brain ischemia in mice. J Neurochem. 2009;110:12–22.
47. Pinteaux E, Rothwell NJ, Boutin H. Neuroprotective actions of endogenous interleukin-1 receptor antagonist (IL-1ra) are mediated by glia. Glia. 2006;53:551–6.
48. Nishimura M, Izumiya Y, Higuchi A, Shibata R, Qiu J, Kudo C, et al. Adiponectin prevents cerebral ischemic injury through endothelial nitric oxide synthase dependent mechanisms. Circulation. 2008;117:216–23.
49. Song W, Huo T, Guo F, Wang H, Wei H, Yang Q, et al. Globular adiponectin elicits neuroprotection by inhibiting NADPH oxidase-mediated oxidative damage in ischemic stroke. Neuroscience. 2013;248:136–44.
50. Birkeland KI, Hanssen KF, Torjesen PA, Vaaler S. Level of sex hormone-binding globulin is positively correlated with insulin sensitivity in men with type 2 diabetes. J Clin Endocrinol Metab. 1993;76:275–8.
51. Tao C, Sifuentes A, Holland WL. Regulation of glucose and lipid homeostasis by adiponectin: effects on hepatocytes, pancreatic β cells and adipocytes. Best Pract Res Clin Endocrinol Metab. 2014;28:43–58.
52. Schwenk RW, Dirkx E, Coumans WA, Bonen A, Klip A, Glatz JF, et al. Requirement for distinct vesicle-associated membrane proteins in insulin- and AMP-activated protein kinase (AMPK)-induced translocation of GLUT4 and CD36 in cultured cardiomyocytes. Diabetologia. 2010;53:2209–19.
53. Simó R, Saez-Lopez C, Lecube A, Hernandez C, Fort JM, Selva DM. Adiponectin upregulates SHBG production: molecular mechanisms and potential implications. Endocrinology. 2014;155:2820–30.
54. Glotov, A.S., Tiys, E.S., Vashukova, E.S., Pakin, V.S., Demenkov, P.S., Saik, O.V. et al. Molecular association of pathogenetic contributors to pre-eclampsia (pre-eclampsia associome). BMC Syst Biol. 2015;9 Suppl 2:S4.
55. Kzhyshkowska J, Workman G, Cardó-Vila M, Arap W, Pasqualini R, Gratchev A, et al. Novel function of alternatively activated macrophages: stabilin-1-mediated clearance of SPARC. J Immunol. 2006;176:5825–32.
56. Noy PJ, Lodhia P, Khan K, Zhuang X, Ward DG, Verissimo AR, et al. Blocking CLEC14A-MMRN2 binding inhibits sprouting angiogenesis and tumour growth. Oncogene. 2015;34:5821–31.
57. Conway CD, Howe KM, Nettleton NK, Price DJ, Mason JO, Pratt T. Heparan sulfate sugar modifications mediate the functions of slits and other factors needed for mouse forebrain commissure development. J Neurosci. 2011;31:1955–70.
58. Guo L, Wang L, Li H, Yang X, Yang B, Li M, et al. Down regulation of GALNT3 contributes to endothelial cell injury via activation of p38 MAPK signaling pathway. Atherosclerosis. 2016;245:94–100.
59. Remus EW, O'Donnell RE, Rafferty K, Weiss D, Joseph G, Csiszar K, et al. The role of lysyl oxidase family members in the stabilization of abdominal aortic aneurysms. Am J Physiol Heart Circ Physiol. 2012;303:H1067–75.